J Therm Anal Calorim (2013) 111:1203–1210
DOI 10.1007/s10973-012-2346-y

Experimental study of Fe–C–O based system below 1000 °C

Monika Žaludová · Bedřich Smetana · Simona Zlá · Jana Dobrovská · Vlastimil Vodárek · Kateřina Konečná · Vlastimil Matějka · Petra Matějková

CEEC-TAC1 Conference Special Issue

Abstract The paper deals with the study of phase transformation temperatures of Fe (Fe–C–O) based metallic alloys. Six model alloys with graded carbon and oxygen content were used for experimental investigation. Low-temperature region (<1000 °C) was the investigated area. Phase transformation temperatures were obtained using Differential thermal analysis and Setaram Setsys 18_{TM} laboratory system. Controlled heating was conducted at the rates of 2, 4, 7, 10, 15, 20 °C min^{-1}. Region of eutectoid transformation ($Fe_{\alpha(C)} + Fe_3C \rightarrow Fe_{\gamma(C)}$), alpha–gamma ($Fe_{\alpha(C)} \rightarrow Fe_{\gamma(C)}$) and transformation $Fe_{\alpha(O)} + Fe_{0.92}O \rightarrow Fe_{\gamma(O)} + Fe_{0.92}O$ was studied. New original data (phase transformation temperatures) were obtained in this study. The relationship between shift of phase transformation temperatures and chemical composition (mainly carbon and oxygen content) is investigated in this paper. To achieve good approximation to the equilibrium conditions, the extrapolation of the obtained phase transformation temperatures to the zero heating rate was performed. The influence of experimental conditions (heating rate) on temperatures of phase transformations was studied as well. Comparison of the obtained experimental data with the data presented in the accessible literature and IDS calculations (Solidification Analysis Package) was carried out. It follows from literature search that there is a lack of thermo-physical and thermo-dynamical data on Fe–C–O system.

Keywords: Fe–C–O system · DTA · Transformation temperatures · Zero heating rate

M. Žaludová (✉) · B. Smetana · S. Zlá · J. Dobrovská
Faculty of Metallurgy and Materials Engineering, Department of Physical Chemistry and Theory of Technological Processes, VŠB-TU Ostrava, 17. listopadu 2172/15, Ostrava-Poruba, Czech Republic
e-mail: monika.zaludova@vsb.cz

V. Vodárek · K. Konečná
Faculty of Metallurgy and Materials Engineering, Department of Materials Engineering, VŠB-TU Ostrava, 17. listopadu 2172/15, Ostrava-Poruba, Czech Republic

V. Matějka · P. Matějková
Nanotechnology Centre, VŠB-TU Ostrava, 17. listopadu 2172/15, Ostrava-Poruba, Czech Republic

Introduction

Iron based alloys are important materials, however, still a lack of experimental material data describing thermo-physical and thermo-dynamical properties of these alloys exist. That is why these alloys are still subject of extensive research. This paper deals with the study of phase transformations temperatures of Fe–C–O based metallic alloys in the eutectoid and alpha–gamma region. Insufficient quantity of thermo-physical and thermo-dynamical data about this system is available at present. For example the ASM international database of phase diagrams [1] contains only two isothermal sections through the ternary phase diagram of the system Fe–C–O, namely for the temperatures of 400 and 600 °C. (The same database contains more than 100 ternary diagrams for the Fe–C–Cr system) Important data are for example temperatures and latent heats of phase transformations, heat capacities [2], surface tension. It is possible to find in available literature values of some of the above physical quantities for the Fe–C [3] and Fe–O [4] systems, however even these available data differ [5]. One of the possibilities of obtaining the necessary data is use of computational relations [6] or simulation (computational) programmes [7], such as IDS software for calculation of phase transformation temperatures and other material properties of steels and Fe–C based alloys [8, 9].

Differential thermal analysis (DTA) [10, 11] was used for obtaining the temperatures of phase transformations for six Fe–C–O based alloys in low-temperature region. Experimental measurements were carried out using the Setaram SETSYS 18_{TM} experimental equipment.

The newly obtained data will serve for completion of the existing thermo-physical data on the system Fe–C–O, and they can subsequently contribute also to a clearer description and easier understanding of more complex poly-component systems, like for example steels [5].

Theoretical background

At present there is insufficient quantity of thermo-physical and thermo-dynamical data on the system Fe–C–O. That is why the binary systems Fe–C and Fe–O, for which substantially more data are contained in literature, were in this study taken as a basis for investigation of the Fe–C–O system.

Fe–C System

Two important phase transformations take place in Fe–C system in the low-temperature region [3]. When the critical temperature, characterised by the GS curve (Fig. 1) is exceeded (cooling), alpha ferrite starts to precipitate from austenite. Alpha ferrite is paramagnetic above the temperature of 760 °C (temperature of Curie point), below this temperature it is getting ferromagnetic properties. At the temperature of 723 °C precipitation of ferrite is terminated and austenite with eutectoid concentration decomposes to a mixture of ferrite and cementite (P), see the straight line OS (Fig. 1). At the temperature, characterised by the OQ curve (Fig. 1), tertiary cementite (Fe_3C_{III}) starts to precipitate from alpha ferrite.

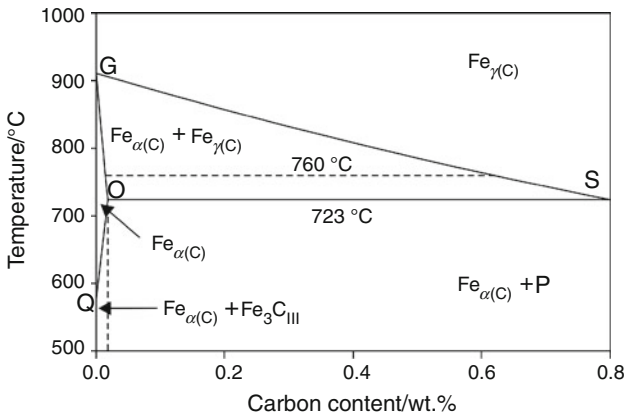

Fig. 1 Fe–C metastable equilibrium diagram

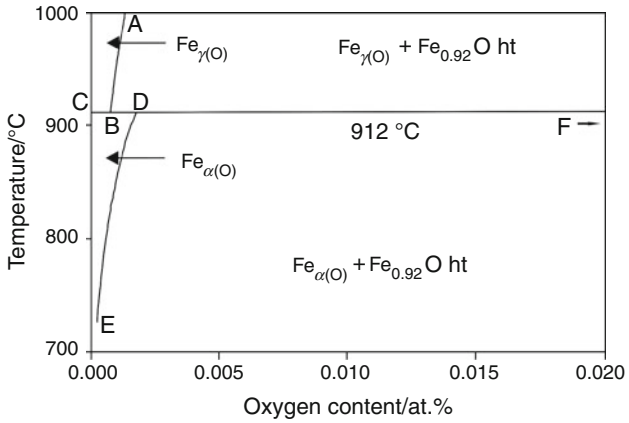

Fig. 2 Fe–O equilibrium phase diagram

Fe–O System

Several important phase transformations run in the low-temperature area of the Fe–O system (Fig. 2) [4]. During cooling first occurs precipitation of $Fe_{0.92}O$ from Fe_γ in conformity with the curve AB. At the temperature of 912 °C three phase transformations run in dependence on oxygen concentration. $Fe_{\gamma(O)}$ is in the concentration range from 0 to 0.0008 at % O transformed to $Fe_{\alpha(O)}$, see the straight line CB. In the concentration range from 0.0008 to 0.0017 at % O a transformation of $Fe_{\gamma(O)}$ to $Fe_{\alpha(O)}$ takes place, as well as dissolution of $Fe_{0.92}O$, see the straight line BD. $Fe_{\gamma(O)}$ is in the range from 0.0017 to ~50 at % O transformed to $Fe_{\alpha(O)}$ at presence of $Fe_{0.92}O$, see the straight line DF. $Fe_{0.92}O$ precipitates from $Fe_{\alpha(O)}$ according to the straight line DE.

More information can be found for example in [12, 13]. The temperatures of phase transformations and concentration ranges, in which individual transformations run, differ from each other.

Experiment

Samples characterisation

Fe based alloys with graded carbon and oxygen content, prepared in laboratory, were studied. Samples of Fe–C–O alloys were prepared by vacuum melting of ingots made of plasma prepared iron with addition of graphitic carbon. Chemical composition of the Fe plasma is given in Table 1 (Fe_{pl}). During the melting the added carbon reacted with oxygen, that was present in the plasma prepared iron, creating oxide of carbon (CO with high probability). The more carbon was added during vacuum melting, the more oxygen reacted with carbon, creating thus oxide of carbon (it was manifested also by an increase of pressure in

Table 1 Chemical composition of analysed samples

Sample	Composition/wt %									Composition/at %	
	C	O	Mn	Si	P	S	Cr	Ni	V	C	O
Fe_{pl}	0.010	0.110	0.042	0.005	0.002	0.004	0.004	0.015	0.022	0.0464	0.3828
1	0.002	0.043	0.021	0.005	0.004	0.008	0.003	0.026	0.012	0.0093	0.1499
2	0.004	0.088	0.009	0.004	0.004	0.007	0.002	0.023	0.007	0.0185	0.3065
3	0.005	0.038	0.026	0.006	0.004	0.008	0.003	0.024	0.013	0.0232	0.1325
4	0.038	0.002	0.025	0.014	0.004	0.008	0.004	0.026	0.015	0.1765	0.0070
5	0.167	0.0005	0.020	0.007	0.004	0.008	0.003	0.025	0.013	0.7719	0.0017
6	0.197	0.0004	0.022	0.019	0.004	0.008	0.004	0.024	0.017	0.9096	0.0014

Table 2 Comparison of characteristic temperatures obtained by DTA and DSC, 4 °C min^{-1}

Sample	Method	Temperature/°C						
		T_{EUT}	T_C	$T_{\alpha-\gamma,\ S}$	$T_{\alpha-\gamma,\ E}$	$T_{Fe\alpha-Fe\gamma(O)}$	T_D	$T_{Fe\alpha-Fe\gamma}$
2	DTA		768.5	908.9		915.1		
	DSC		768.6	909.1		914.3		
4	DTA		768.7		918.4			
	DSC	735.0	769.1		917.2			
6	DTA	733.7	768.3		854.3		909.1	919.6
	DSC	734.9	769.1		853.0		910.9	919.1

vacuum furnace). Chemical composition of the analysed samples is given in Table 1. Chemical composition of samples was determined using spectrometer with spark discharge. Carbon and oxygen content in samples was determined using combustion analysers. The samples for DTA analysis were processed into the form of cylinders with diameter of 3.5 mm and height of ~3 mm. Mass of the cylinders was ~150 mg.

Experimental conditions

Setaram SETSYS 18_{TM} (TG/DTA/DSC/TMA) laboratory system for thermal analysis and DTA 'S' type (Pt/PtRh 10%) measuring rod were used for obtaining of phase transformation temperatures. The samples were analysed in corundum crucibles with volume of 100 µl. An empty corundum crucible served as reference. Dynamic atmosphere of Ar (purity > 99.9999%) was maintained in furnace during analysis to protect the sample against oxidation. Each alloy was analysed at the controlled heating rates of 2, 4, 7, 10 15, 20 °C min^{-1}.

Reference measurements were performed with samples 2, 4 and 6 with use of the DSC method [14] and Netzsch STA 449 F3 Jupiter equipment at the same experimental conditions. Reference measurements were performed at only one heating rate (4 °C min^{-1}). Small thermal effects became less distinct. Comparison of temperatures of phase transformations (Table 2) obtained by DTA and DSC methods showed very good agreement (differences no more than 2 °C).

IDS

The IDS software (Solidification Analysis Package) was also used for calculation of phase transformation temperatures. This software enables calculation of phase transformation temperatures of Fe–C based systems depending not only on the chemical composition, but also on the cooling rate and the dendrite arm diameter. In the interval below 1000 °C the software also takes into account the influence of the austenitic grain size and the influence of austenitization after solidification. Calculation of phase transformation temperatures assumes some simplifications, such as e.g.: regular dendritic structure, perfect solubility in liquid phase, thermodynamic equilibrium at interfacial boundaries and some other simplifications and limitations are also applied [8]. Certain suitable concentration interval for every element is recommended by authors. Concentration interval for oxygen is 0.0–0.001 wt % and for carbon is 0.05–1.2 wt %. If the element content is entered outside the given range, the calculated values of temperatures may (need not) be unrealistic. This is also the case of some calculated temperatures of samples analysed in this study. Calculation of temperatures comprised concentrations of all elements present in the analysed samples (Table 1). The maximal possible value of oxygen content

enabling to start the calculation for sample 2 was 0.044 wt % (0.044 wt % is the maximum possible concentration for starting the calculation). The cooling rate used for calculation was 0.06 °C min^{-1}. (In order to achieve the best possible approximation to the equilibrium temperatures.) Although eutectoid phase transformation runs at one temperature, for the reasons of non-equilibrium conditions the IDS programme calculated for this transformation a temperature range.

Results and discussion

Temperatures of phase transformations were obtained on the basis of DTA curves (Fig. 3) evaluation. Figure 3 shows DTA curves obtained for the analysed Fe–C–O samples at the heating rate of 2 °C min^{-1}. Evolution of individual DTA curves differs in dependence on carbon and oxygen content in the samples.

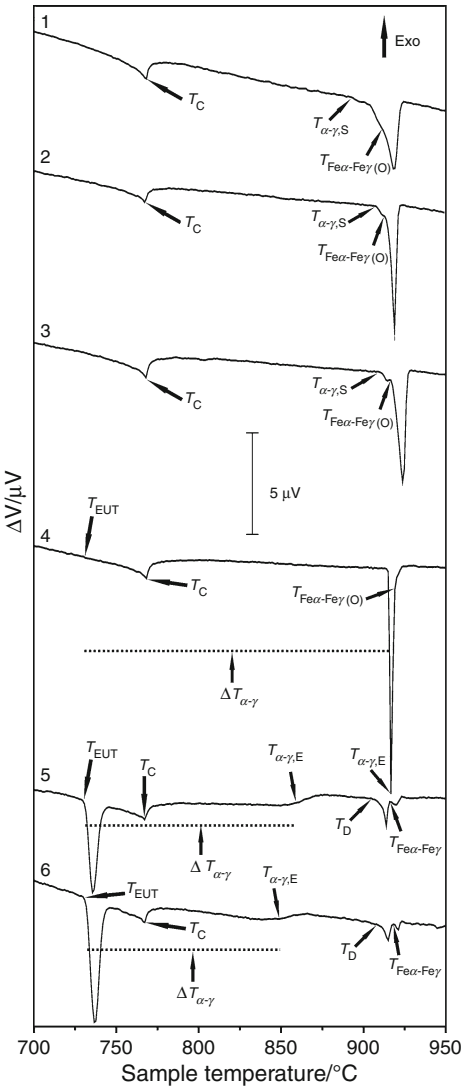

Fig. 3 DTA curves of the analysed samples, heating rate 2 °C min^{-1}

Eutectoid phase transformation ($Fe_{\alpha(C)} + Fe_3C \rightarrow Fe_{\gamma(C)}$) takes place in the samples 4, 5, 6 (Fig. 3). The samples 1, 2, 3 have low carbon content, and for this reason no eutectoid phase transformation took place in them (Fig. 3). Temperature of eutectoid phase transformation is marked as T_{EUT}. Thermal effect of eutectoid phase transformation increases with the increasing carbon content. Thermal effect in the sample 4 is very small. At low heating rates (2 and 4 °C min^{-1}) the thermal effect in the sample 4 was not detected. (Temperature marked as T_{EUT} for sample 4 (Fig. 3) is temperature calculated for the zero heating rate.)

Magnetic transition was detected in all samples. Temperature of Curie point T_C was obtained.

Alpha–gamma phase transformation ($Fe_{\alpha(C)} \rightarrow Fe_{\gamma(C)}$) takes place in a wide temperature range (731–917 °C; temperature range was taken from temperature values calculated for the zero heating rate) for samples 4–6 and in a narrow temperature range for samples 1–3 (893–919 °C). Start of this transformation is marked as $T_{\alpha-\gamma,\,S}$. Temperature range marked as $\Delta T_{\alpha-\gamma}$, is the range, in which transformation runs, and end of transformation is marked as $T_{\alpha-\gamma,\,E}$. $T_{\alpha-\gamma,\,S}$ is identical to the temperature T_{EUT} for samples 4–6. $T_{\alpha-\gamma,\,E}$ is identical to the temperature $T_{Fe\alpha-Fe\gamma(o)}$ for samples 1–3.

Transformation $Fe_{\alpha(O)} + Fe_{0.92}O \rightarrow Fe_{\gamma(O)} + Fe_{0.92}O$ runs in the samples 1–4. Temperature of this transformation is marked as $T_{Fe\alpha-Fe\gamma(o)}$.

Probably, the $Fe_{0.92}O$ in the samples 5 and 6 dissolves and solid solution of $Fe_{\alpha(O)}$ forms (T_D) and afterwards the transformation $Fe_{\alpha(O)} \rightarrow Fe_{\gamma(O)} + Fe_{0.92}O$ ($T_{Fe\alpha-Fe\gamma}$) takes place. Marking of characteristic temperatures is for clarity summarised in Table 3.

On the basis of Fe–O and Fe–C system knowledge the possible phase transformations were assigned to the observed thermal effects. In the samples 1, 2, 3, 4 two thermal effects occur on DTA curves in the narrow temperature range (of ~890–930 °C). The phase

Table 3 Labeling of characteristic temperatures

T_{EUT}	Temperature of eutectoid transformation $Fe_{\alpha(C)} + Fe_3C \rightarrow Fe_{\gamma(C)}$
T_C	Temperature of magnetic transition (Curie point)
$T_{\alpha-\gamma,\,S}$	Temperature of start of transformation $Fe_{\alpha(C)} \rightarrow Fe_{\gamma(C)}$
$\Delta T_{\alpha-\gamma}$	Temperature range of transformation $Fe_{\alpha(C)} \rightarrow Fe_{\gamma(C)}$
$T_{\alpha-\gamma,\,E}$	Temperature of end of transformation $Fe_{\alpha(C)} \rightarrow Fe_{\gamma(C)}$
$T_{Fe\alpha-Fe\gamma(O)}$	Temperature of transformation $Fe_{\alpha(O)} + Fe_{0.92}O \rightarrow Fe_{\gamma(O)} + Fe_{0.92}O$
T_D	Temperature of start of transformation $Fe_{\alpha(O)} + Fe_{0.92}O \rightarrow Fe_{\alpha(O)}$
$T_{Fe\alpha-Fe\gamma}$	Temperature of transformation $Fe_{\alpha(O)} \rightarrow Fe_{\gamma(O)} + Fe_{0.92}O$

transformations $Fe_{\alpha(C)} \rightarrow Fe_{\gamma(C)}$ and $Fe_{\alpha(O)} + Fe_{0.92}O \rightarrow Fe_{\gamma(O)} + Fe_{0.92}O$ were assigned to thermal effects, on the basis of interpretation of Fe–C and Fe–O diagrams [3, 4] and also on the basis of magnitude of thermal effect of the relevant transformation and carbon or oxygen content in the sample. Assignment of these transformations to individual thermal effects assumes the presence of two phases-solid solution of oxygen in iron and solid solution of carbon in iron. The same assumption was applied for the thermal effects assignment in the samples 5 and 6 also. Succession of individual transformations is schematically presented in Table 4.

Characteristic transformation temperatures are shown in Tables 5, 6, 7, 8, 9, 10. Small thermal effects (for example thermal effects corresponding to the transformation $Fe_{\alpha(C)} \rightarrow Fe_{\gamma(C)}$ in the samples 1–3) were observed only at lower heating rates (2 and 4 °C min^{-1}). At lower heating rates the overlapping thermal effects are separated. At higher heating rates so small thermal effects weren't detected, that is why characteristic temperatures of these transformations for higher heating rates are not given in Tables 5, 6, 7, 8, 9, 10.

It is evident from the results given in Tables 5, 6, 7, 8, 9, 10, that heating rate influences the shift of temperatures of phase transformations. Temperatures of phase transformations are shifted with an increasing heating rate towards higher temperatures. The shift varies within an order of units of °C. This can be explained particularly by process dynamics and by detection capability of the device. Different rates of the process of heating/cooling could have also substantial influence on kinetics of the phase transformations. In general, phase transformation mechanism could change with changing heating/cooling rate. Phase transformations may be for this reason at various rates detected at various temperatures (in various temperature intervals) [15].

Table 4 Scheme of succession of transformations of samples

Samples 1–3	$Fe_{\alpha(C,\ O)ferromagnetic} \rightarrow Fe_{\alpha(C,\ O)paramagnetic}$
	$Fe_{\alpha(C)} \rightarrow Fe_{\gamma(C)}$
	$Fe_{\alpha(O)} + Fe_{0.92}O \rightarrow Fe_{\gamma(O)} + Fe_{0.92}O$
Sample 4	$Fe_{\alpha(C)} + Fe_3C \rightarrow Fe_{\gamma(C)}$
	$Fe_{\alpha(C,\ O)ferromagnetic} \rightarrow Fe_{\alpha(C,\ O)paramagnetic}$
	$Fe_{\alpha(C)} \rightarrow Fe_{\gamma(C)}$
	$Fe_{\alpha(O)} + Fe_{0.92}O \rightarrow Fe_{\gamma(O)} + Fe_{0.92}O$
Samples 5, 6	$Fe_{\alpha(C)} + Fe_3C \rightarrow Fe_{\gamma(C)}$
	$Fe_{\alpha(C,\ O)ferromagnetic} \rightarrow Fe_{\alpha(C,\ O)paramagnetic}$
	$Fe_{\alpha(C)} \rightarrow Fe_{\gamma(C)}$
	$Fe_{\alpha(O)} + Fe_{0.92}O \rightarrow Fe_{\alpha(O)}$
	$Fe_{\alpha(O)} \rightarrow Fe_{\gamma(O)} + Fe_{0.92}O$

Table 5 Experimental temperatures of phase transformations and temperatures calculated for the zero heating rate for sample 1

Heating rate/°C min^{-1}	Temperature/°C		
	T_C	$T_{\alpha-\gamma,\ S}$	$T_{Fe\alpha-Fe\gamma(O)}$
2	768.1	892.9	909.7
4	768.5	893.1	908.4
7	768.8		908.3
10	769.6		910.3
15	769.5		911.4
20	770.6		912.9
0	768.0		906.5

Table 6 Experimental temperatures of phase transformations and temperatures calculated for the zero heating rate for sample 2

Heating rate/°C min^{-1}	Temperature/°C		
	T_C	$T_{\alpha-\gamma,\ S}$	$T_{Fe\alpha-Fe\gamma(O)}$
2	768.1	908.4	915.5
4	768.5	908.9	915.1
7	768.7		916.5
10	769.7		915.1
15	770.3		917.6
20	771.2		917.9
0	767.7		914.6

Table 7 Experimental temperatures of phase transformations and temperatures calculated for the zero heating rate for sample 3

Heating rate/°C min^{-1}	Temperature/°C		
	T_C	$T_{\alpha-\gamma,\ S}$	$T_{Fe\alpha-Fe\gamma(O)}$
2	768.3	910.7	917.6
4	768.6	913.3	921.0
7	768.4		921.1
10	769.5		922.8
15	771.0		923.2
20	771.1		923.0
0	767.8		919.0

Extrapolation of temperatures to the zero heating rate

In order to minimize the influence of experimental conditions (heating rate), the temperatures of phase transformations, obtained at heating, were extrapolated to the zero heating rate. The temperatures for the zero heating rate approach the temperatures of phase transformations at equilibrium conditions. More detailed explanation related to the equilibrium temperatures of phase transformations is given for example in [16].

Table 8 Experimental temperatures of phase transformations and temperatures calculated for the zero heating rate for sample 4

Heating rate/°C min^{-1}	Temperature/°C			
	T_{EUT}	T_C	$T_{\alpha-\gamma,\ E}$	$T_{Fe\alpha-Fe\gamma(O)}$
2		768.2	917.6	919.0
4		768.7	918.4	
7	734.5	769.3	919.6	
10	735.5	768.5	919.5	
15	737.5	770.3	922.1	
20	740.6	772.3	924.1	
0	731.0	767.6	916.8	

Table 9 Experimental temperatures of phase transformations and temperatures calculated for the zero heating rate for sample 5

Heating rate/°C min^{-1}	Temperature/°C				
	T_{EUT}	T_C	$T_{\alpha-\gamma,\ E}$	T_D	$T_{Fe\alpha-Fe\gamma}$
2	731.5	767.7	862.9	910.8	915.9
4	732.6	768.1	865.2	911.6	918.9
7	733.6	768.5	870.9		
10	735.3	769.6	873.3		
15	736.4	769.7	875.3		
20	737.5	770.3	878.2		
0	731.3	767.6	863.0		

Table 10 Experimental temperatures of phase transformations and temperatures calculated for the zero heating rate for sample 6

Heating rate/°C min^{-1}	Temperature/°C				
	T_{EUT}	T_C	$T_{\alpha-\gamma,\ E}$	T_D	$T_{Fe\alpha-Fe\gamma}$
2	732.5	767.7	854.3	910.1	918.2
4	733.7	768.3	854.3	909.1	919.6
7	734.8	768.5	862.8		
10	736.6	769.3	864.1		
15	737.1	769.3	865.8		
20	739.2	769.7	871.7		
0	732.2	767.8	853.0		

Comparison with accessible data

Temperatures of phase transformations obtained for the zero heating rate (in some cases for 2 °C min^{-1}) were compared with the equilibrium metastable Fe–C diagram (Fig. 4), with the equilibrium Fe–O diagram (Fig. 5), and with the temperatures calculated by the programme IDS (Table 11).

Figure 4 presents a comparison of experimentally obtained temperatures of phase transformations with the equilibrium metastable Fe–C diagram. Experimentally obtained temperatures are in this diagram plotted in dependence on the carbon content (wt %). Carbon content in the samples 1–3 is very similar (low), for this reason only the temperatures for sample 1 are given in the diagram

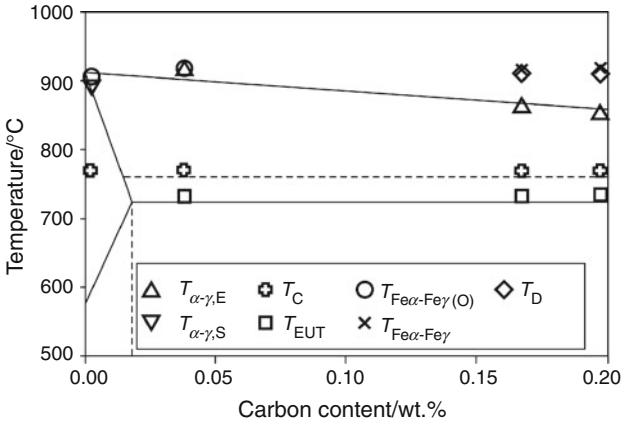

Fig. 4 Comparison of zero heating rate temperatures with the metastable equilibrium diagram Fe–C for samples 1, 4–6

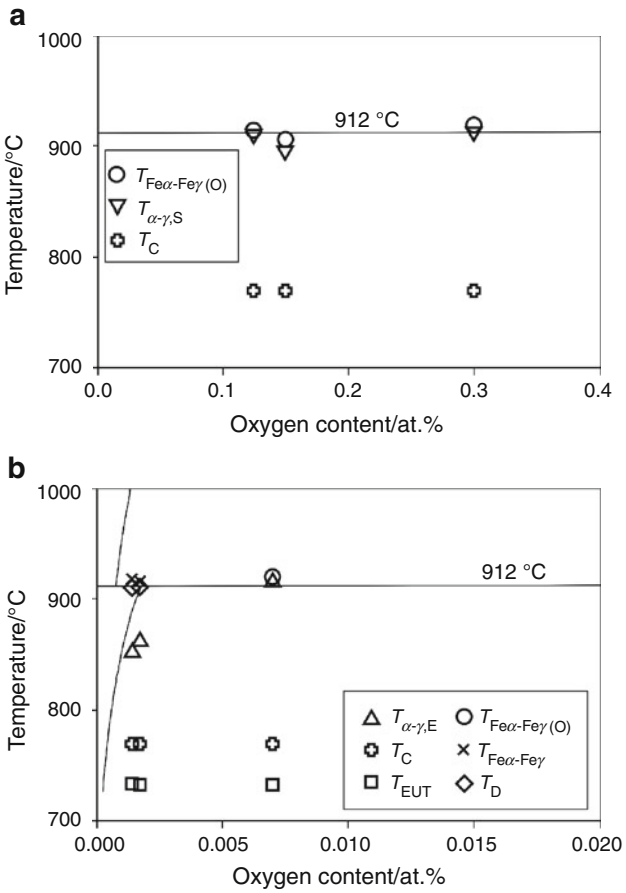

Fig. 5 Comparison of zero heating rate temperatures with the equilibrium diagram Fe–O for **a** samples 1–3 with higher oxygen content **b** for samples 4–6 with lower oxygen content

Table 11 Comparison of the phase transformations temperatures for the zero heating rate with the temperatures calculated by IDS software

Sample	Temperature/°C						
	Eutectoid			Curie		Alpha–Gamma	
	Exp.	IDS start	IDS end	Exp.	IDS	Exp. end	IDS *Ae*3
1				768.0			941.6
2				767.7			939.0
3				767.8			934.6
4	731.0	771.0	751.0	767.6	768.0	916.8	902.2
5	731.3	749.8	729.8	767.6	768.0	863.0	852.5
6	732.2	745.9	725.9	767.8	768.0	853.0	843.9

for clarity. In the case of temperatures (T_{EUT}, T_C, $T_{\alpha-\gamma,\ S}$, $T_{\alpha-\gamma,\ E}$) it was a very good agreement achieved. Differences between experimentally obtained temperatures and temperatures given in the Fe–C diagram are of the order of °C. Higher difference between the temperatures was found only for $T_{\alpha-\gamma,\ E}$ of the sample 4 ($\sim$15 °C).

The fact that experimentally obtained temperatures of eutectoid phase transformation and Curie temperature are higher in comparison with Fe–C diagram, is probably caused by content of other elements in the samples (Table 1), particularly by content of oxygen.

Figure 5 shows comparison of experimentally obtained temperatures of phase transformations with an equilibrium Fe–O diagram. The experimentally obtained temperatures are in this diagram plotted in dependence on oxygen content in the samples. Oxygen content in the samples varies within the range from 0.0004 to 0.088 wt % O (0.0014–0.3065 at %). Due to different oxygen content in the samples (difference of an order), two cuts of Fe–O phase diagram were selected. Comparison of experimentally obtained temperatures of phase transformations with the phase diagram Fe–O showed a good agreement in the case of temperatures $T_{Fe\alpha-Fe\gamma(O)}$, $T_{Fe\alpha-Fe\gamma}$, T_D. The differences between experimentally obtained temperatures and temperatures presented in the Fe–O diagram were of the order of centigrades. Higher difference between temperatures was observed only at the transformation $Fe_{\alpha(O)} + -Fe_{0.92}O \rightarrow Fe_{\alpha(O)}$ in the sample 5, namely $\sim$20 °C.

Experimental temperatures were obtained at the heating mode, contrary to that the temperatures calculated using IDS software for cooling mode. The experimental temperatures of eutectoid transformation lay in the temperature range calculated by the programme IDS (Table 11). Only the temperature of eutectoid transformation of the sample 4 is lower ($\sim$ by 20 °C) than the lower limit of the temperature range, in which the eutectoid transformation runs according to the IDS programme. Temperatures of the end of alpha-gamma phase transformation obtained in this study are higher than temperatures *Ae*3 (equilibrium temperature of formation of pro-eutectoid ferrite) calculated by the programme IDS (by more than 10 °C).

It follows from obtained results that the prepared Fe–C–O samples exhibit characteristic features of both Fe–C and Fe–O system. This is evident from the comparison of experimental values of phase transformation temperatures with presented equilibrium phase diagrams (Figs. 4, 5).

Conclusions

Six model alloys with graded carbon and oxygen content were investigated by the DTA and Setaram Setsys 18_{TM} laboratory system. Low-temperature region (below 1,000 °C) of the Fe–C–O system was the investigated area. Phase transformation temperatures were obtained. New original data (phase transformation temperatures) of the Fe–C–O system in the low-temperature region were obtained. Succession of phase transformation was suggested for all the samples.

In order to minimize the influence of experimental conditions (heating rate), the temperatures of phase transformations were extrapolated to the zero heating rate. The temperatures obtained for the zero heating rate were compared with the equilibrium Fe–C diagram, with the equilibrium Fe–O diagram and with the temperatures calculated by IDS software. In majority of transformations temperature differences of the order of units of °C were observed. Influence of carbon and oxygen content (chemical composition) on temperatures of phase transformations was assessed also.

It follows from literature search that there is a lack of thermo-physical and thermo-dynamical data on Fe–C–O system.

The Fe–C–O system will be still subject of extensive research at our working site.

Acknowledgements The study was carried out in the scope of the projects of the Czech Science Foundation (107/11/1566 and 106/08/0606) and the project No. CZ.1.05/2.1.00/01.0040 "Regional Materials Science and Technology Centre" within the frame of the operation programme 'Research and Development for Innovations' financed by the Structural Funds and from the state budget of the Czech Republic and of the student's project entitled 'Selected studies of heterogeneous systems' (SP2011/17), and it was financed from the specific research resources of the Faculty of Metallurgy and Materials Engineering, VSB-Technical University of Ostrava, Czech Republic.

References

1. Villars P, Okamoto H, Cenzual K (2006) ASM Alloy Phase Diagrams Center. ASM International, Materials Park, OH. http://www1.asminternational.org/AsmEnterprise/APD

2. Raju S et al. (2010) Drop calorimetry studies on 9Cr-1 W-0.23 V-0.06Ta-0.09C reduced activation steel. Int J Thermophys. doi:10.1007/s10765-010-0720-1
3. Ryš P, Cenek M, Mazanec K, Hrbek A (1975) Material science I, Metal science 4, 1st edn. ACADEMIA, Praha
4. Sundman B (1991) An assessment of the Fe–O system. J Phase Equilib. doi:10.1007/BF02645709
5. Smetana B et al. (2010) Phase transformation temperatures of pure iron and low alloyed steels in the low temperature region using DTA. Int J Mater Res. doi:10.3139/146.110283
6. Cabrera-Marrero JM et al. (1998) Macro-micro modeling of the dendritic microstructure of steel billets processed by continuous casting. ISIJ Int. doi:10.2355/isijinternational.38.812
7. Emadi D et al. (2005) Applications of thermal analysis in quality control of solidification processes. J Therm Anal Calorim. doi:10.1007/s10973-005-0772-9
8. Miettinen J (1999) Solidification analysis package for steels—user's manual of DOS version, 1st edn. Helsinky University of Technology, Helsinky
9. Miettinen J (1996) Calculation of solidification-related thermophysical properties for steels. Metall Mater Trans B. doi:10.1007/s11663-997-0095-2
10. Boettinger WJ, et al. DTA and heat-flux DSC measurements of alloy melting and freezing. 1st ed. Washington: National Institute of Standards and Technology; 2006.
11. Gallagher PK. Handbook of thermal analysis and calorimetry: principles and practice. 2nd ed. Oxford: Elsevier; 2003.
12. Wriedt HA (1991) The Fe–O (iron–oxygen) system. J Phase Equilib. doi:10.1007/BF02645713
13. Bjorkman B (1985) An assessment of the system Fe–O–SiO_2 using a structure based model for the liquid silicate. CALPHAD. doi:10.1016/0364-5916(85)90012-4
14. Petrovič DS et al. (2011) Differential scanning calorimetry study of the solidification sequence of austenitic stainless steel. J Therm Anal Calorim. doi:10.1007/s10973-011-1375-2
15. Kempen ATW, Sommer F, Mittemeijer EJ (2002) The kinetics of the austenite-ferrite phase transformation of Fe–Mn: differential thermal analysis during cooling. Acta Mater. doi:10.1016/S1359-6454(02)00149-0
16. Zhao JC. Methods for phase diagram determination. 1st ed. Oxford: Elsevier; 2007.